Journal of Power Sources 226 (2013) 313–319

Contents lists available at SciVerse ScienceDirect

Journal of Power Sources

journal homepage: www.elsevier.com/locate/jpowsour

# In-situ X-ray diffraction studies of lithium–sulfur batteries

Natalia A. Cañas [a,b,*], Steffen Wolf [a], Norbert Wagner [a], K. Andreas Friedrich [a,b]

[a] *Institute of Technical Thermodynamics, German Aerospace Center, 70569 Stuttgart, Germany*
[b] *Institute for Thermodynamic and Thermal Engineering, University of Stuttgart, Germany*

## HIGHLIGHTS

- ► Structural changes of lithium–sulfur batteries were studied by means of in-situ XRD.
- ► Dilithium sulfide was detected the first time at a depth of discharge of 60%.
- ► Sulfur recrystallizes with an orientated structure and lower crystallite size.
- ► Sulfur and dilithium sulfide were semi-quantitatively determined.

## ARTICLE INFO

*Article history:*
Received 2 August 2012
Received in revised form
9 October 2012
Accepted 29 October 2012
Available online 7 November 2012

*Keywords:*
Lithium–sulfur
Battery
In-situ
X-ray diffraction

## ABSTRACT

In order to optimize the cycling performance of lithium–sulfur (Li–S) batteries, it is highly important to understand the structural and morphological changes of the sulfur cathode under operating conditions. In this work, a suitable cell for in-situ X-ray diffraction (XRD) analysis was designed to study the structural modifications on the cathode of Li–S batteries during electrochemical cycling. As a result, the formation of reaction products during charging and discharging was monitored in operando. The formation of dilithium sulfide ($Li_2S$) and the recrystallization of sulfur during the first cycle could be identified. Moreover, these crystalline phases were semi-quantitatively determined by means of XRD analysis. Morphology changes of the cathode due to electrochemical cycling were characterized using scanning electron microscopy (SEM).

## 1. Introduction

Due to its high theoretical capacity (1672 mAh $g_{sulfur}^{-1}$) and energy density (2500 Wh $kg^{-1}$), lithium–sulfur batteries have attracted widespread attention in the battery research community. Further advantages are the low cost and non-toxicity of sulfur. Nevertheless, a known problem of lithium–sulfur batteries is the gradual decrease of discharge capacity during cycling. This is mainly caused by the low electrical conductivity of sulfur and dilithium sulfide, and the formation of soluble polysulfides in the electrolyte. In order to react electrochemically, sulfur has to be in contact with an electrical conductive material (like carbon black, graphite or carbon nanotubes). The morphology of the cathode can change upon cycling and the formerly well-dispersed sulfur can aggregate and become isolated for further reaction. Furthermore, polysulfides of high order ($Li_2S_n$ with $4 \leq n \leq 8$) dissolve in the electrolyte and can diffuse to the anode and react directly with lithium metal. This so-called shuttle mechanism causes irreversible loss of sulfur [1–3]. The polysulfide discharge product, $Li_2S$, is insoluble in the electrolyte and can precipitate on the surface of electrodes, acting as an insulator and avoiding further electrochemical reactions.

In order to understand the degradation mechanisms of this battery, the application of in-situ techniques is necessary. An important characterization method to follow structural and composition changes in a battery during cycling is the analysis by means of X-ray diffraction. In the past, in-situ XRD experiments were already performed successfully on lithium-ion batteries, for example in Refs. [4–10]. So far, however, there has been little application of this method in Li–S batteries [11,12]. In a recent research [12], the formation of the discharge product $Li_2S$ was not detected in operando conditions. In contradiction to these results, we find, that dilithium sulfide does build up during the first discharge cycle. It is important to highlight that dilithium sulfide is a difficult substance to investigate, because it hydrolyzes easily in air, producing $H_2S$ and LiOH. Probable reasons why $Li_2S$ has not

---

[*] Corresponding author. Institute of Technical Thermodynamics, German Aerospace Center, 70569 Stuttgart, Germany. Tel.: +49 0711 6862 576; fax: +49 0711 6862 474.
*E-mail address:* natalia.canas@dlr.de (N.A. Cañas).

0378-7753/$ – see front matter © 2012 Elsevier B.V. All rights reserved.
http://dx.doi.org/10.1016/j.jpowsour.2012.10.092

been detected before are I) the in-situ cell is not airtight, II) the discharge capacity of the cell is too low, $Li_2S$ does not precipitate and only soluble polysulfides are present at discharge state or III) the penetration depth of the X-ray is not high enough and the structural information is only from a deeper region of the bulk cathode material, giving no information from the interface cathode/separator, where probably the main quantity of $Li_2S$ is present.

In this paper, the reactions of crystalline phases in the Li–S battery were monitored for the discharging and charging process by means of in-situ XRD. The formation of dilithium sulfide and the recrystallization of sulfur have been identified. In addition, this work is complemented with semi-quantitative analysis of the species and SEM characterization of the cathode surface.

## 2. Experimental

### 2.1. Cathode preparation

The cathodes consisted of 50 wt.% sulfur (99.5%, Alfa Aesar), 40 wt.% Super P conductive carbon black (99%, Alfa Aesar) and 10 wt.% polyvinylidene fluoride (PVDF, Alfa Aesar).

First, sulfur and carbon black were mixed for 12 h in a tumbling mixer. PVDF was dissolved in a 50/50 vol.% mixture of dimethyl sulfoxide (DMSO, 99.9%, Sigma Aldrich) and ethanol (99.5%, VWR). All chemical compounds were finally mixed together for 6 h.

The suspension was sprayed by use of an air-atomizing external mixing nozzle (LECHLER GmbH) controlled by a 3D axis robot. Each cathode was prepared by spraying four layers over a 6 μm thick aluminum collector. Between each spraying, the cathode was dried in an oven at 60 °C. The drying step improves the adherence of the cathode coating on the aluminum collector and the homogeneity of the layers. The thickness of the cathode layer, without substrate, varied between 15 μm and 20 μm.

### 2.2. In-situ cell

The in-situ cell consists of two holed aluminum plates, the cathode plate with a thin aluminum window and the anode plate. The aluminum window is fixed onto the cathode plate with a conductive epoxy. Each plate acts as electrode collector and can be connected directly to the potentiometer inserting banana jacks in the hole located in each plate of the cell. A plastic tube is placed in the middle of the cell to insulate electrically the battery from the interior walls of the cell. In order to seal the cell airtight, a 0.75 mm thick polymer gasket is positioned between the two plates. Additionally, this avoids an internal short circuit between both electrode plates. A metal spring inside the cell applies mechanical pressure of the stack (see Fig. 1, components 5–8) against the Al-window. An exploded illustration of the cell composition is shown in Fig. 1.

### 2.3. Assembling of the cell

The battery was assembled in a Glove Box under Argon atmosphere. The 1.5 mm thick lithium anode (99.9%, Sigma Aldrich) was placed on an aluminum disk over the spring. The separator, a 25 μm thick polypropylene microporous membrane (Celgard 2500), was set on top of the anode and soaked with 14 μL electrolyte, 1 M $LiPF_6$ (99.99%, Sigma Aldrich) in tetraethylene glycol dimethyl ether (TEGDME, 99.9%, Sigma Aldrich). The cathode was placed on the separator. The cell-stack was positioned in the in-situ cell and this was finally closed with plastic screws. The diameter of the lithium foil and cathode was 10 mm, while the separator diameter was 2 mm larger dimensioned to avoid short circuit. We used a thin Al-foil of 6 μm thick that allows us to obtain information until the separator surface. Fig. 8, Ia, b shows SEM pictures of the cathode before cycling. It can be seen that the sulfur particles were covered with the carbon black nanoparticles.

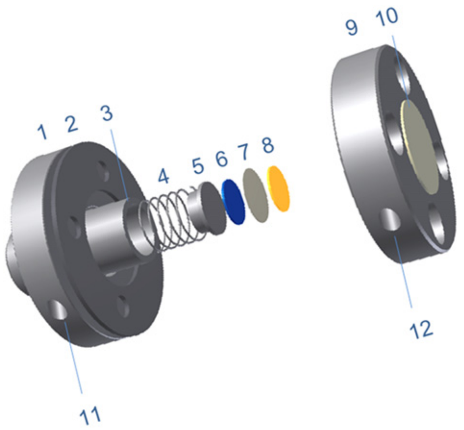

**Fig. 1.** Exploded illustration of the in-situ XRD cell. 1) Anode plate, 2) polymer gasket, 3) insulator plastic tube, 4) spring, 5) Al-anode collector, 6) anode, 7) separator, 8) cathode, 9) cathode plate, 10) Al-window and 11–12) holes for connecting the banana jacks.

### 2.4. Electrochemical cycling, X-ray diffraction and scanning electron microscopy

The cycling performance of the battery was investigated by use of a Zahner® IM6 electrochemical workstation, with the battery measurement software Zahner® Thales [13]. The charge–discharge procedure was carried out in galvanostatic mode at a current density of 300 mA $g_{sulfur}^{-1}$ in a voltage range between 2.8 V and 1.5 V. Once the charge end voltage of 2.8 V was reached, a potentiostatic period followed for 15 min before starting the next cycle.

X-ray diffractograms were recorded with an X-ray diffractometer, D8 Discover GADDS, equipped with a VÅNTEC-2000 area detector. Exposures were made in reflexion mode with a tuned monochromatic and parallel X-ray beam (Cu-$K_\alpha$), with a tube collimator aperture of 1 mm. The accelerating voltage was 45 kV and the tube current was 0.650 mA. Each diffraction pattern was measured in four frames with a step size of 23°, starting with $\theta_1 = \theta_2 = 12°$ (Bragg–Brentano condition). The exposure time for each frame was 180 s.

Twelve minutes were required to record each in-situ XRD pattern. The electrochemical testing of the cell was not stopped neither during charging nor discharging. For this reason, the XRD pattern represents averaged values of the reflected X-ray during the exposure time.

The morphological changes on the cathode surface were observed in SEM (Zeiss ULTRA plus with Charge Compensation). The accelerating voltage was 1 kV and the secondary electron detector was used.

## 3. Results and discussion

### 3.1. Discharge cycle

Fig. 2 shows the X-ray patterns measured at different depth of discharge (DOD, %) during the first galvanostatic discharge. Thereby, only the range of interest of the diffraction patterns ($2\theta = 20°–35°$) is shown. The Bragg peaks of sulfur can be clearly detected in the first spectrum (Power Diffraction File [14], PDF, number: 00-008-0247). The structure of sulfur is orthorhombic face centered, which is the stable modification of sulfur below 96 °C